Large Multiple Transmembrane Domain Fragments of a G Protein-Coupled Receptor: Biosynthesis, Purification, and Biophysical Studies

Zhanna Potetinova,[1] Subramanyam Tantry,[1] Leah S. Cohen,[1] Katrina E. Caroccia,[1,2] Boris Arshava,[1] Jeffrey M. Becker,[3] Fred Naider[1,2]

[1]*Department of Chemistry, College of Staten Island, The City University of New York, Staten Island, NY 10314*

[2]*Department of Biochemistry, The Graduate Center of the City University of New York, NY*

[3]*Department of Microbiology, University of Tennessee, Knoxville, TN 37996*

Received 6 February 2012; revised 1 June 2012; accepted 2 July 2012
Published online 17 July 2012 in Wiley Online Library (wileyonlinelibrary.com). DOI 10.1002/bip.22122

ABSTRACT:

To conduct biophysical analyses on large domains of GPCRs, multimilligram quantities of highly homogeneous proteins are necessary. This communication discusses the biosynthesis of four transmembrane and five transmembrane-containing fragments of Ste2p, a GPCR recognizing the Saccharomyces cerevisiae *tridecapeptide pheromone α-factor. The target fragments contained the predicted four N-terminal Ste2p[G_{31}-A_{198}] (4TMN), four C-terminal Ste2p[T_{155}-L_{340}] (4TMC), or five C-terminal Ste2p[I_{120}-L_{340}] (5TMC) transmembrane segments of Ste2p. 4TMN was expressed as a fusion protein using a modified pMMHa vector in L-arabinose-induced* Escherichia coli *BL21-AI, and cleaved with cyanogen bromide. 4TMC and 5TMC were obtained by direct expression using a pET21a vector in IPTG-induced* E. coli *BL21(DE3) cells. 4TMC and 5TMC were biosynthesized on a preparative scale, isolated in multimilligram amounts, characterized by MS and investigated by biophysical methods. CD spectroscopy indicated the expected highly α-helical content for 4TMC and 5TMC in membrane mimetic environments. Tryptophan fluorescence showed that 5TMC integrated into the nonpolar region of 1-stearoyl-2-hydroxy-*sn*-glycero-3-phospho-(1′-*rac*-glycerol) micelles. HSQC-TROSY investigations revealed that [^{15}N]-labeled 5TMC in 50% trifluoroethanol-d_2/H_2O/0.05%–trifluoroacetic acid was stable enough to conduct long multidimensional NMR measurements. The entire Ste2p GPCR was not readily reconstituted from the first two and last five or first three and last four transmembrane domains.* © *2012 Wiley Periodicals, Inc. Biopolymers (Pept Sci) 98: 485–500, 2012.*

Keywords: membrane protein fragments; GPCR; protein expression; CD of membrane polypeptides; direct expression

This article was originally published online as an accepted preprint. The "Published Online" date corresponds to the preprint version. You can request a copy of the preprint by emailing the Biopolymers editorial office at biopolymers@wiley. com

Additional Supporting Information may be found in the online version of this article.

Correspondence to: Fred Naider, Department of Chemistry, College of Staten Island, The City University of New York, Staten Island, NY 10314 USA;
e-mail: fred.naider@csi.cuny.edu

Contract grant sponsor: NIH
Contract grant number: GM22087

INTRODUCTION

G protein-coupled receptors (GPCRs) are a superfamily of signal transducing membrane proteins found in eukaryotes that play important physiological roles in signaling, regulatory, and metabolic processes.[1,2] Defects in these membrane proteins cause a number of serious disorders that result in disease.[3] More than one third

of the therapeutic drugs on the market today are known to be human GPCR agonists or antagonists.[4] Therefore, a better understanding of GPCR structure, function, and mechanism of action would play a key role in therapeutic development. Except for rhodopsin, expression levels of GPCRs in their native cells are quite low and to reach the mg levels needed for crystallization or NMR studies heterologous expression is necessary.

Despite their important roles, some aspects of GPCR biology remain under described. Atom-level high-resolution information about ligand binding, and ligand-receptor interactions became available only recently.[5–20] Nearly all of these studies are on highly modified proteins which, in many cases, contain an inserted T4 lysozyme to aid crystallization. Moreover, the X-ray structures reveal little about the highly dynamic nature of these very flexible signal transduction proteins. Although there is no sequence homology between the six subfamilies, all GPCRs have a common heptahelical structure, analogous signal transduction mechanisms and are believed to undergo conformational changes upon ligand binding.[21–24] Class A (rhodopsin-like family) GPCRs have been the most extensively studied at atomic resolution due to success in obtaining several members in sufficient quantities and purity to obtain crystals.[5–10,13,14,16,18] Heteronuclear NMR methods used to generate high-resolution protein structures require incorporation of $^{15}N/^{13}C/^{2}H$ isotopes into the target structure. Of the ~1000 GPCRs identified in the genome, only the human vasopressin V2,[25] cannabinoid 2 (CB2),[26] and most recently, CXCR1[27] receptors have been isolated in an isotope-labeled form in the multimilligram quantities needed for NMR. High-resolution solution structures were recently solved for the GPCR analogues sensory rhodopsin II[28] and proteorhodopsin[29]; however, these proteins are significantly smaller than mammalian GPCRs. Thus, even with the recent advances in NMR, structural and dynamical investigations remain challenging and approaches for the efficient expression of isotopically labeled GPCRs are needed. In contrast to intact GPCRs, fragments (~20–120 residues) of some GPCRs have been studied by multidimensional NMR.[30] Most NMR studies have been on fragments containing a single transmembrane (TM) segment, with several reports on two-TM fragments including human CB2, CB1, and Y4 receptors.[31–35] Our group has also reported NMR structures in organic-aqueous media and LPPG micelles for TM1-TM2 of Ste2p, a yeast GPCR.[36,37]

The study of fragments as surrogates for structural studies on regions of GPCRs presumes that these regions assume structures that reflect those in the intact protein. Support for this assumption comes from *in vitro* and *in vivo* GPCR reconstitution studies,[38–43] which demonstrated that fragments recognize each other and assemble into a biologically and biochemically functional protein. Our studies on TM1-TM2 of Ste2p, a 431-residue α-factor pheromone receptor from the yeast *Saccharomyces cerevisiae,* which belongs to the fungal mating pheromone GPCR class D,[44] indicated that this 80-residue polypeptide folded into a structure that was a two-helix hairpin in detergent micelles. However, to fully validate this structure it is necessary to study the two-TM fragment in the context of a receptor reconstituted from segmentally labeled fragments. Thus this study addresses the biosynthesis and biophysical characterization of four and five TM constructs of Ste2p (TM1-TM4, TM4-TM7, and TM3-TM7) for eventual use in reconstitution experiments.

Previously Ste2p fragments, containing from one to three TM helices, were successfully expressed by our laboratory with and without fusion proteins in amounts sufficient for high-resolution NMR investigations.[37,45–49] Here, we tested two biosynthetic approaches: (1) the TrpΔLE fusion protein, typically used and (2) a direct expression strategy. The 221-residue five TM Ste2p fragment (5TMC) was heterologously expressed directly in unlabeled and labeled forms in a high yield and homogeneity. 5TMC was examined in membrane-mimetic environments for structural stability by different biophysical methods. Sample conditions were identified for high-resolution NMR investigations of 5TMC in an organic-aqueous medium. The propensity of Ste2p fragments to assemble spontaneously into Ste2p like heterodimers in micelles was evaluated. The biosynthetic approaches developed herein should be applicable to the preparation of other hydrophobic and difficult-to-express membrane proteins for use in biophysical investigations and provide the requisite tools for the eventual reconstitution of Ste2p from 2TMN and 5TMC.

MATERIALS AND METHODS

Materials

Chemicals were purchased from Sigma-Aldrich (St. Louis, MO) if not specified otherwise. HPLC grade water, 2-propanol, and methanol were obtained from JT Baker (Phillipsburg, NJ), acetonitrile from Spectrum (New Brunswick, NJ). *Escherichia coli* (*E. coli*) growth media and reagents were obtained from Sigma-Aldrich and from Becton, Dickinson and Company (Franklin Lakes, NJ). The SuperSignal West Pico kit for detection of polyhistidine proteins with HisProbe-HRP was obtained from Pierce (Rockford, IL), Coomassie Blue was from BioRad (Hercules, CA). The detergents dodecylphosphocholine (DPC), 1-myristoyl-2-hydroxy-*sn*-glycero-3-phospho-(1′-*rac*-glycerol) (LMPG), 1-palmitoyl-2-hydroxy-*sn*-glycero-3-phospho-(1′-*rac*-glycerol) (LPPG), and 1-stearoyl-2-hydroxy-*sn*-glycero-3-phospho-(1′-*rac*-glycerol) (LSPG) were obtained from Avanti Polar Lipids (Alabaster, AL). 1,1,1,3,3,3-Hexafluoroisopropanol-d_2 (HFIP-d_2, 98%) was purchased from Cambridge Isotope Laboratories (Andover, MA).

Construction of the GPCR Plasmids

The DNA plasmids encoding Ste2p[I_{120}-L_{340}] (5TMC) and Ste2p[T_{155}-L_{340}] (4TMC) regions with an octahistidine tag at the

N-terminus were constructed using PCR with the template pMD1732, obtained from Mark Dumont. They were created from pMD354 plasmid[42] by site-directed mutagenesis[50] converting naturally occurring Met residues to Ile or Leu (M54I, M69I, M71I, M165I, M180I, M189I, M218L, and M294I). The amplified PCR products (primer sequences can be found in Supporting Information Table S1) were digested with *Nde*I and *Bam*HI and subcloned into a pET21a expression vector (Novagen). Finally, the M250I mutation was introduced into the Met- and Cys-less constructs using a modification of the Stratagene Quikchange mutagenesis protocol (Stratagene, La Jolla, CA). The DNA fragment encoding the Ste2p[G_{31}-A_{198}] (4TMN) region as a TrpΔLE fusion protein with a nonahistidine tag at the N-terminus of the fusion was cloned into a modified pMMHa plasmid,[44] pSW02.[45] The gene was amplified from pMD1732 using the primers in Supporting Information Table S1. The generated PCR fragment and vector DNA were digested with *Hind*III and *Bam*HI enzymes.

After digestion with restriction enzymes, the purified PCR products were ligated into the appropriately prepared expression vectors with T4 DNA ligase. PCR oligonucleotides, restriction enzymes, T4 ligase, and Platinum *Pfx* DNA polymerase were purchased from Invitrogen (Grand Island, NY) and used according to the manufacturer's instructions. All DNA plasmids were prepared using the Wizard® Plus SV Minipreps DNA purification system (Promega, Madison, WI) and stored at −20°C. Correct inserts into the vectors were confirmed by screening with double restriction enzyme analysis. The fidelity of the modified receptor constructs was checked by sequencing (the University of Tennessee DNA Sequencing Core Facility).

Protein Expression

The resulting plasmids encoding the four and five TM domain fragments cloned above were transformed into different *E. coli* BL21 expression strains, purchased as competent cells from Invitrogen, following the manufacturer's procedures. The expression was performed in rich (Luria Broth, LB) or minimal (M9: 20 m*M* KH_2PO_4, 48 m*M* Na_2HPO_4, 8.6 m*M* NaCl, 2 m*M* $MgSO_4$, 0.1 m*M* $CaCl_2$, 0.1% NH_4Cl, and 0.4% glucose[51]) medium supplemented with appropriate antibiotics. Expression in M9 medium was also performed using $^{15}NH_4Cl$ to produce isotopically labeled peptide. In the case of BL21(DE3) and BL21-AI cells, ampicillin was used at a final concentration of 200 mg/L. For BL21(DE3)pLysS and BL21Star(DE3)pLysS strains, a liter of the culture medium was supplemented with both, 200 mg ampicillin and 34 mg chloramphenicol.

Single colonies or 5 μL from a fresh transformation reaction were inoculated into 10 mL of LB, and cells were grown overnight at 37°C (∼16 h). Then the overnight cultures were diluted 1:50 with fresh LB medium and incubated to the desired OD_{600}. To optimize expression conditions, the typical small-scale experiment was performed in a 250 mL flask with 50 mL of medium. Large-scale experiments were carried out in 4 L flasks with 1 L of medium. Optimization in minimal medium was performed as above, but the 50 mL LB cultures were harvested by centrifugation at ∼1200*g* for 20 min when they reached the desired OD_{600}, the pellets were resuspended in the same volume of M9 medium and then induced. All DE3 strains were induced with 0.125–1.0 m*M* isopropyl-β-D-thiogalactopyranoside (IPTG), whereas the expression in BL21-AI was induced with 0.5% L-arabinose with or without 1 m*M* IPTG. The small-scale induced cultures were incubated at different temperatures 37, 30, or 20°C for 18–22 h. Uninduced and induced 1 mL samples were collected at different post-induction times for SDS-PAGE analysis, centrifuged at 2040*g* for 15 min, and prepared using an inclusion body protocol for analytical samples, as described below, to evaluate protein expression levels. At the end of the fermentation processes, the growth cultures were centrifuged at 3400*g* (small-scale) or 3800*g* (large-scale) for 25 min, the supernatant was removed and the pellets were stored at −20°C (small-scale) or −70°C (large-scale) for further use.

Purification of GPCR Fragments

Inclusion Body Preparation. Inclusion bodies (IBs) were isolated as described previously for one and two TM domain-containing fragments with some modification.[52] All protocol steps were performed at 4°C or on ice. Sonication was carried out using a Sonicator 3000 (Misonix, Farmingdale, NY) instrument equipped with a Cup Horn sonicator head, and a circulating ice-water bath (4–5°C) to reduce sample heat.

The pellets from the 1 mL analytical samples collected during the expression optimizations were suspended in 0.2 mL of lysis buffer (50 m*M* Tris-HCl and 1 m*M* ethylenediaminetetraacetic acid, pH 8.7) containing 1 m*M* phenylmethylsulfonylfluoride and 0.3 mg/mL lysozyme and incubated for at least 15 min in an ice bath. Then the lysed cell suspension was sonicated and centrifuged at 21,100*g* for 20 min. The supernatant was carefully removed, and the pellets were washed in the same manner with 1% mild detergent (lysis buffer containing 1% igepal Ca-630 and 1% deoxycholic acid) and then water. During each step, the pellets were homogenized with sonication and centrifuged as describe above. The isolated IBs were resuspended in 0.1 mL of SDS-PAGE loading buffer (50 m*M* Tris-HCl, pH 6.8 containing 4% SDS, 12% glycerol, and Coomassie Brilliant Blue G) by sonication in a room temperature water bath, and 20-μL samples were analyzed by SDS-PAGE.

Small-scale pellets from 50-mL growth culture were suspended in 1 mL of lysis mixture [lysis buffer containing 1 m*M* phenylmethylsulfonylfluoride, 0.3 mg/mL lysozyme, 5 m*M* $MgSO_4$, 5 m*M* dithiothreitol (DTT) and 2.4 U/mL benzonase]. After incubation for 30 min in an ice bath, the suspension was sonicated and centrifuged at 21,100*g* for 30 min. The supernatant was carefully poured off, and the pellets were sequentially treated with 1 mL of lysis buffer containing 5 m*M* DTT, 1 mL of 1% mild detergent, and 1 mL of water and kept at −20°C.

Large-scale 1 L growth pellets were treated with 8 mL of lysis mixture, followed by 8 mL of lysis buffer containing 5 m*M* DTT, 6 mL of 1% mild detergent, and 4 mL of water as described above for the small-scale samples. After sonication in an ice-water bath, the pellets were centrifuged at 39,000*g* for 20–40 min. Finally, the isolated IBs were resuspended in 8 mL of water, aliquoted in 1 mL (5TMC) or 2 mL (4TMC) portions for an HPLC purification step, centrifuged at 21,100*g* for 1 h, decanted, and left at −20°C. The supernatants from each step were collected and analyzed by HPLC and Western blot for the presence of the desired protein.

HPLC Analysis and Purification. Separation was performed on an Agilent 1100 HPLC system using Zorbax 300SB-C3 analytical (4.6 × 150 mm; 3.5-μm) or preparative (21.2 × 150 mm; 7-μm) columns at 60°C with monitoring at 220 nm. To prepare an analytical HPLC sample, IBs isolated from 0.25 to 0.5 mL culture, were dis-

solved in 80 μL of trifluoroacetic acid (TFA), sonicated for 10 sec, and diluted with 20 μL of H_2O. An 80 μL sample was analyzed by HPLC at a flow rate of 1 mL/min with a linear gradient 60–98% of 90% acetonitrile/10% isopropanol/0.1%TFA (eluent B) over 30 min using 90% water/10% isopropanol/0.1% TFA as eluent A. The large hydrophobic membrane fragments could not be eluted completely after a primary injection. To recover as much polypeptide as possible, we used 2–3 post-elution injections with 80% TFA/H_2O and ran the identical gradient as above. The HPLC peak corresponding to a desired compound was collected from the primary and post-injections; the fractions were combined and lyophilized.

The preparative purification was carried out at a flow rate of 5 mL/min with sequential linear gradients of eluent C, 80% acetonitrile/20% isopropanol/0.1% TFA, (5TMC: 55–68% C for 15 min, 68–85% C for 30 min, and 85–98% C for 5 min; 4TMC: 50–98% C for 50 min) against eluent D, 80% water/20%isoproanol/0.1% TFA. The isolated IBs from 125 mL (for 5TMC) or 250 mL (for 4TMC) cultures were dissolved in 0.9 mL of TFA, sonicated for 10–15 sec, diluted with 0.1 mL of H_2O and immediately injected into the HPLC. HPLC fractions containing the desired polypeptides were lyophilized and analyzed by MALDI-TOF and Western blot.

SDS-PAGE, Western Blotting, and Mass Spectrometry (MALDI-TOF)

The proteins were separated on a 16% SDS-PAGE gel as described[53] and stained with Coomassie Brilliant Blue G-250 or R-250. To perform Western blot experiments, proteins were separated into bands using electrophoresis, transferred to a nitrocellulose membrane using a Trans-Blot SD semi-dry transfer cell (BioRad), blocked with Bovine Serum Albumin (10 mg/mL) at 13°C overnight, and incubated in the HisProbe-HRP solution (Pierce) for 1 h at room temperature. MALDI-TOF spectra were recorded on Microflex Bruker (Billerica, MA) equipment with a sinapinic acid (SA) or α-cyano-4-hydroxycinnamic acid (CHCA) matrix dissolved in 70% acetonitrile/30% [H_2O/0.1%TFA].

Cleavage of 4TMN Fusion Protein

The 4TMN-FP IBs from 1-mL cell pellets were dissolved in 160 μL TFA by sonication for 10 sec at room temperature and diluted with 40 μL H_2O. Then the solution was added to 29 mg of cyanogen bromide, the reaction mixture was vortexed, and left in the dark for 2 h. An 85 μL sample was injected into the analytical HPLC system and analyzed with a 70–98% linear gradient of eluent B for 30 min as described above.

Circular Dichroism (CD) Spectroscopy

CD measurements were performed on an AVIV Model 410 CD spectropolarimeter (AVIV Biomedical, Lakewood, NJ) at 25°C. The final concentration of the GPCR fragments was 10 μ*M*. The protein concentrations were determined spectrophotometrically at 280 nm in a Thermo Electron Corporation (Waltham, MA) Helios Beta UV–visible spectrophotometer using extinction coefficients of 13,590 M^{-1} cm^{-1} for 5TMC and 12,250 M^{-1} cm^{-1} for 4TMC.[54] CD spectra were acquired from 250 to 185 nm with an interval of 1 nm, a bandwidth of 1 nm, and a 1 sec integration time at each wavelength. Each CD spectrum represents the average of at least three scans and was corrected by subtraction of a background solvent spectrum without the protein. A quartz cuvette of 1.0 mm path length was used for proteins in organic-aqueous solvents. The GPCR fragments were first dissolved in organic solvent, sonicated for 5 min (TFE) or 3 min (HFIP) at room temperature, and diluted with water. The CD samples in micelles were prepared using a protocol similar to that previously used to prepare samples of Ste2p fragments for NMR analysis.[55] The protein (2 nmol) and a detergent (4 μmol) were dissolved in 0.3 mL of HFIP, the solution was sonicated for 10 min at 50°C and lyophilized for at least 18–20 h. Then the mixture was suspended in 0.2 mL of 20 m*M* phosphate buffer, pH 5.6 by vortexing for 10–20 sec and incubated for 15 min at 37°C. The final concentration of detergent was 20 m*M*. This concentration was above the critical micelle concentration (CMC) for every detergent tested. To compare the peptide in various solvents a stock solution was used and all samples were prepared by aliquoting the peptide from this stock solution. This gave a very good control of the relative concentrations. A 0.5 mm path length quartz cuvette was used for the experiments with micelles. The ellipticity is reported as mean residue ellipticity ($[\theta_{222}]$, deg cm^2 $dmol^{-1}$). Fraction helicity was calculated using the following equation,

$$f_H = ([\theta]_{222} - [\theta]^0{}_{222})/([\theta]^{100}{}_{222} - [\theta]^0{}_{222})$$

where f_H represents fraction helicity, $[\theta]_{222}$ represents the mean residue ellipticity at 222 nm, $[\theta]^{100}{}_{222}$ represents the mean residue ellipticity at 222 nm for a 100% helical protein and is estimated to be 30,000 deg cm^2 $dmol^{-1}$, and $[\theta]^0{}_{222}$ represents the mean residue ellipticity at 222 nm for a random coil protein and is estimated to be 2000 deg cm^2 $dmol^{-1}$.[56,57]

NMR Spectroscopy

For preparation of NMR samples, 1.5 mg of the [^{15}N]-uniformly labeled 5TMC fragment was dissolved in 175 μL of TFE-d_2 by sonication for 5 min at room temperature, 175 μL of H_2O/0.1%TFA was added, and the solution was transferred to a Shigemi NMR tube (Shigemi, Allison Park, PA). A similar procedure was used for samples at different percentages of TFE-d_2 or HFIP-d_2 in H_2O. The NMR spectra were recorded on a Varian VNMRS DirectDrive 600-MHz NMR spectrometer (Varian NMR Instrument, Palo Alto, CA) equipped with a Cryo Probe. All spectra were recorded at 45°C. The total acquisition times of the [^{15}N,^{1}H]-HSQC[58] or −HSQC-TROSY[59] spectra were from 2 to 14 h. ^{1}H spectra in TFE/H_2O have been referenced by assigning the methylene proton peak of TFE as having a chemical shift of 3.88 ppm. ^{1}H spectra in HFIP/H_2O were referenced using DSS as a standard at 0 ppm. ^{15}N chemical shifts in 2-D HSQC experiments were calibrated indirectly using chemical shifts ratio coefficient 0.101329118.[60,61]

Fluorescence Spectroscopy

Fluorescence data were obtained on a JY-Horiba (Edison, NJ) *Fluoromax-3* spectrofluorimeter at ambient temperature using an excitation wavelength of 280 nm. The emission spectra were scanned in a 10-mm quartz cuvette from 285 to 500 nm at an interval of 1 nm with a 1 sec integration time at each wavelength. The 5TMC samples in 50% TFE/H_2O or LSPG-containing 20 m*M* phosphate buffer (pH 5.6) were prepared in the same manner as described above for the CD samples. The

Table I Composition and Mutations of the Ste2p Fragments

Name	GPCR Construct		Molecular Mass (Da)[a]	
	Amino acid sequence of the GPCR fragment	Mutations	Theoretical (H^+ average)	Experimental (positive MALDI-TOF)
4TMN-FP	Met-His_9-TrpΔLE-Met-Ste2p (Gly_{31}-Ala_{198})	M54I, C59S, M69I, M71I, K77R, M165I, M180I, and M189I	31684.8	31,683
4TMN	Ste2p (Gly_{31}-Ala_{198})	M54I, C59S, M69I, M71I, K77R, M165I, M180I, and M189I	18307.4	18,308
4TMC	Met-His_8-Ste2p (Thr_{155}-Leu_{340})	M165I, M180I, M189I, M218L, M250I, C252S, and M294I	21374.6	21,399
5TMC	Met-His_8-Ste2p (Ile_{120}-Leu_{340})	M165I, M180I, M189I, M218L, M250I, C252S, M294I, and A299V	25229.2	25,222

[a] The differences observed between the calculated and experimental molecular masses are within the precision of the measurement for large membrane proteins.

fluorescence study in micelles was performed at a final LSPG concentration of 10 m*M*. Each fluorescence emission spectrum was corrected by subtraction of a background spectrum without the protein.

Study of Heterodimer Formation from Ste2p Fragments using SDS-PAGE and MALDI Experiments

5TMC and 2TMN were first dissolved in 100% TFE, sonicated for 10 min at room temperature, and diluted with water to give a final TFE/H_2O ratio of 5/2 (v/v). The protein concentrations were determined by UV at 280 nm using extinction coefficients of 9570 M^{-1} cm^{-1} for 2TMN and 13,590 M^{-1} cm^{-1} for 5TMC.[54] Then the stock solutions were aliquoted to obtain samples with different ratios of 5TMC/2TMN (1/0.5; 1/1; 1/2; and 1/4). After lyophilization, the protein mixtures were resuspended in 20 m*M* phosphate buffer, pH 5.6 containing 20 m*M* SDS by sonication at an output power of 48–50 W at 50°C for 15 min and incubated at 25°C overnight. The concentration of 5TMC was 25 μM. For each sample, 1 μL was analyzed by MALDI-TOF using SA or CHCA matrices. The remaining amount of each sample was lyophilized, resuspended in the same volume of the loading buffer without SDS (50 m*M* Tris-HCl, pH 6.8 containing 12% glycerol, and Coomassie Brilliant Blue G) by vortexing, incubated at 37°C for 15 min and analyzed by SDS-PAGE (Coomasie Brilliant Blue R-250 and Western blotting). Samples of 3TMN and 4TMC mixed at different ratios were prepared similarly using an extinction coefficient of 12,250 M^{-1} cm^{-1} for both Ste2p fragments.[54] [^{15}N]-2TMN (Ste2p[G_{31}-T_{110}, M54L, C59S, M69V, and M71I]) and [^{15}N]-3TMN (Ste2p[G_{31}-R_{161}, M54L, C59S, M69V, and M71I]), used in the study, were prepared previously.[48,49]

RESULTS

Optimization of the Expression of Four and Five TM Domain-Containing GPCR Fragments

The 4TMC, Ste2p[T_{155}-L_{340}], and 5TMC, Ste2p[I_{120}-L_{340}], constructs bearing an N-terminal octahistidine tag, were obtained using a direct expression approach with a pET21a vector. The 4TMN, Ste2p[G_{31}-A_{198}] fragment was fused to the C-terminus of the nonahistidine-tagged TrpΔLE peptide[62,63] and the construct was expressed with a modified pMMHa vector, pSW02.[45] The 4TMN-FP (TrpΔLE-Ste2p[G_{31}-A_{198}]) construct contained a Met residue between the fusion peptide and the Ste2p fragment and mutations of Met and Cys residues to allow for CNBr cleavage. The mutagenesis protocols also resulted in small sequence variations (K77R in 4TMN and A299V in 5TMC; Table I). 4TMC contained 10 residues from I2 beginning at T155, the last 4 contiguous TM domains and 40 residues from the CT tail (Supporting Information Figure S1). 5TMC contained 13 residues from E1 beginning at I120, the last 5 contiguous TM domains, and 40 residues from the CT tail (Supporting Information Figure S1). 4TMN contained 19 residues from the NT tail beginning at G31, the first 4 contiguous TM domains, and 10 residues from E2 (Supporting Information Figure S1). None of the mutations (Table I) were expected to affect the bioactivity of Ste2p based on published data.[64] The Ste2p(A299V) receptor, prepared separately, had wild-type activity in the growth arrest and gene induction assays (data not shown).

Expression of 4TMN as a Fusion Protein. Western blot analysis indicated that all *E. coli* strains tested express the 4TMN fusion in rich medium (Figure 1). The highest expression of 4TMN-FP in rich medium was observed in BL21(DE3) cells (Figure 1, lane 2). Expression in this *E. coli* strain improved in M9 medium where the amount of the desired protein was still high and the level of background expression was slightly lower than in LB medium (Figure 1, compare lanes 2 and 6). In BL21-AI cells, the protein expression level was low in rich medium but significantly higher in minimal medium (Figure 1, lanes 1 and 5). The presence of IPTG had no effect on the expression in BL21-AI cells (data not shown) in contrast to

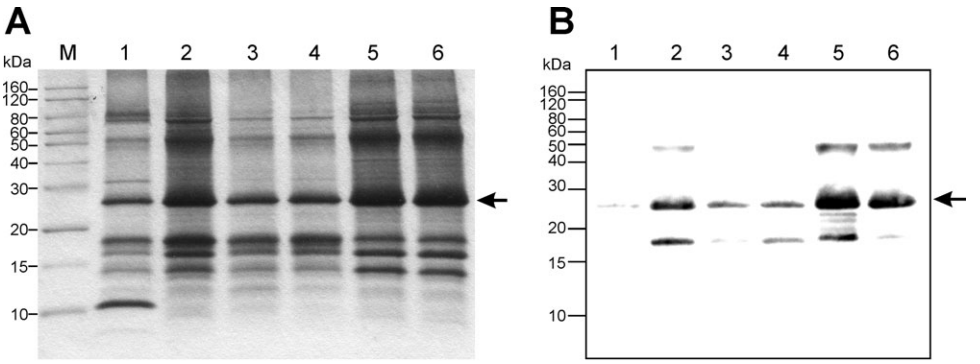

FIGURE 1 Expression of the TrpΔLE-Ste2p[G_{31}-A_{198}] fusion protein (4TMN-FP) in different BL21 cells. Coomassie Blue stained gel (A) and Western blot (B) of the 4TMN-FP IBs expressed at 30°C for 18–21 h. Lane M, molecular-mass markers (BenchMark™, Invitrogen); lanes 1 and 5, BL21-AI; lanes 2 and 6, BL21(DE3); lane 3, BL21(DE3)pLysS; lane 4, BL21Star(DE3)pLysS. The induction OD_{600} was 0.6–0.7 in LB medium (lanes 1–4) or 0.9–1.1 in M9 medium (lanes 5 and 6). The DE3 cells were induced with 1.0 m*M* IPTG. BL21-AI cells were induced with 0.5% L-arabinose. The desired 4TMN-FP has a molecular weight of ~32 kDa (Table I) and is marked with the arrow.

previous results with Ste2p(G_{31}-T_{110}), which was expressed better in the same cells with both IPTG and arabinose.[48] The optimal temperature for 4TMN-FP expression in M9 medium was determined to be 30°C for both strains (Figure 2). The expression was induced at ~0.7 OD_{600} in rich medium and at ~1.0 OD_{600} in minimal medium. The best expression of 4TMN-FP for a 1 L growth under our experimental protocols was obtained using BL21-AI cells, M9 medium, 0.5% L-arabinose, 30°C, and 21 h (Figure 2, panel B). RP-HPLC analysis of the 4TMN-FP IBs isolated under these conditions

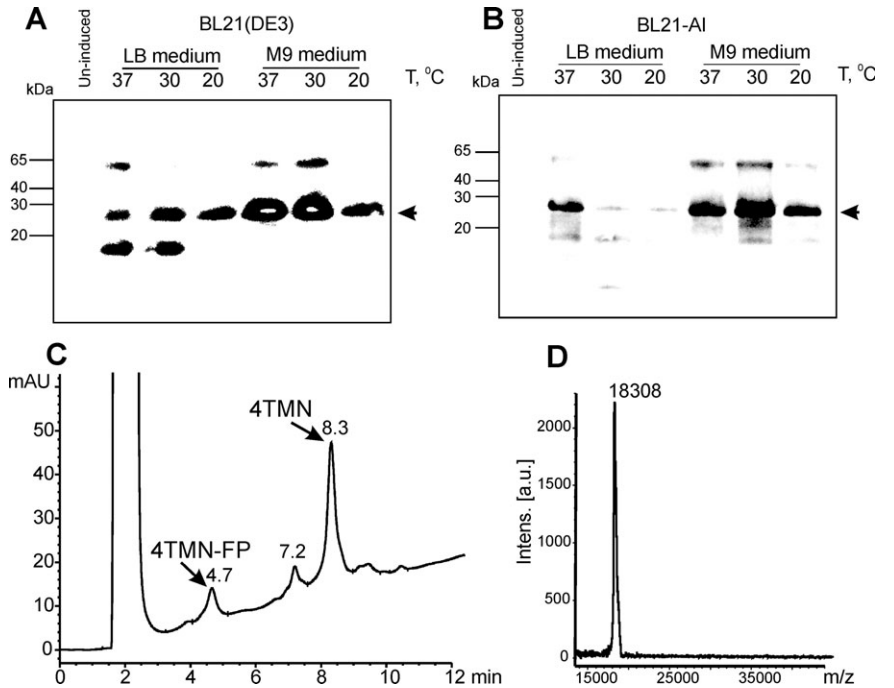

FIGURE 2 Expression and cleavage of TrpΔLE-Ste2p[G_{31}-A_{198}] fusion protein (4TMN-FP). Western blot of the 4TMN-FP IBs expressed in BL21(DE3) (A) or BL21-AI (B) cells at different temperatures. The desired 4TMN-FP has molecular weight of ~32 kDa and is marked with an arrow. RP-HPLC chromatograms of the 4TMN IBs cleaved with CNBr (C). The HPLC gradient was from 60 to 88% eluent B (90% acetonitrile/10% isopropanol/0.1%TFA) where eluent A was 90% water/10% isopropanol/0.1% TFA. (D) Positive MALDI-TOF MS spectrum of HPLC purified 4TMN. Expected molecular weight is 18,307 kDa.

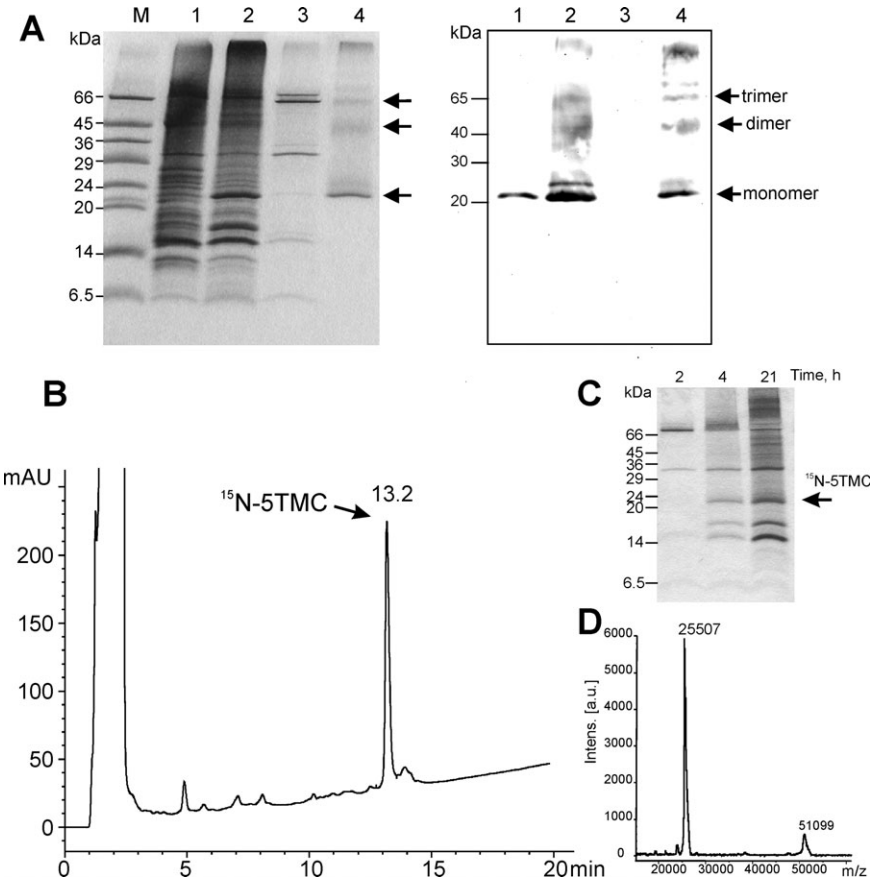

FIGURE 3 Expression and characterization of Ste2p[I_{120}-L_{340}] (5TMC). (A) Coomassie Blue stained gel (left panel) and Western blot (right panel) of the 5TMC IBs expressed in BL21(DE3) cells, LB medium with 1 m*M* IPTG at 37°C (Lane 1), 30°C (Lane 2), and 20°C (Lane 3) for 19–20 h, and HPLC purified 5TMC (Lane 4). Lane M, SigmaMarker™ Low Range protein markers. The desired 5TMC and various oligomers are marked with arrows. HPLC chromatogram (B) and Coomassie Blue stained gel (C) of ^{15}N-labeled 5TMC IBs expressed in BL21(DE3) cells, using M9 medium with 0.25 m*M* IPTG at 30°C for 21 h. The HPLC column was Zorbax 300SB-C3 (4.6 × 150 mm, 3.5-μm). The HPLC gradient was 50–88% eluent B (90% acetonitrile/10% isopropanol/0.1% TFA) where eluent A was 90% water/10% isopropanol/0.1% TFA. (D) Positive MALDI-TOF spectrum of [^{15}N]-labeled 5TMC, purified by HPLC from isolated IBs. Expected molecular weight is 25525 Da for [^{15}N]-labeled 5TMC with 100% incorporation. Observed incorporation was 96% calculated from MALDI-TOF spectra run in parallel for unlabeled ($MW_{observed}$ 25,222 Da; not shown) and [^{15}N]-labeled 5TMC samples.

indicated a single major hydrophobic peak in the HPLC chromatogram (Supporting Information Figure S2A), which corresponds to the desired protein as confirmed by MALDI-TOF MS using a CHCA matrix (Supporting Information Figure S2B). The fusion protein was cleaved with cyanogen bromide in 80% TFA/H_2O to give the target four-domain GPCR fragment. After a 2 h CNBr cleavage, the starting fusion protein was still observed in the reaction mixture (Figure 2C) but longer cleavage time did not improve the yield of 4TMN because the target protein started to degrade. This is consistent with results observed with analogous Ste2p 2TMN and Ste2p 3TMN fusion proteins.[48,49] The released 4TMN was purified by HPLC and characterized by MALDI-TOF MS (Figure 2D).

Direct Expression of 5TMC and 4TMC. To reduce the protein size and post-expression manipulation, 5TMC was biosynthesized using direct expression. For expression in BL21(DE3) in LB, the best protein yield was obtained from growth at 30°C with induction at OD_{600} of 0.7–0.8 (Figure 3A, lane 2). Very little protein was expressed after a 20 h growth at 37°C and 5TMC was not detected at 20°C. The tested pLysS expression strains yielded very small amounts of the protein or did not express at all (data not shown). BL21-AI, when

induced with 0.5% L-arabinose and 1 m*M* IPTG, produced a smaller amount of 5TMC than the BL21(DE3) strain, and expression was slightly reduced with a decrease of IPTG concentration from 1 to 0.125 m*M* in BL21(DE3) at 30°C (data not shown). In M9 minimal medium used for biosynthesis of isotope-labeled compounds, we observed the opposite effect; IPTG concentrations of 0.5 m*M* gave better expression than with 1.0 m*M* IPTG (Supporting Information Figure S3) and 0.25 and 0.125 m*M* IPTG exhibited maximal protein levels (data not shown). The OD_{600}, used for induction, was a critical parameter for expression in minimal medium, as very little expression was observed after inducing a culture with an OD_{600} of ~0.55, but expression increased with induction of a culture with OD_{600} of ~1.0 (Supporting Information Figure S3).

The major hydrophobic peak, found in the HPLC chromatogram of 5TMC IBs (retention time 12–13 min; Figure 3B) was collected, lyophilized, and analyzed by SDS-PAGE, Western blots and MALDI-TOF MS to give a product with the MW expected for 5TMC (25222 Da; Table I). Using the conditions that gave highest expression, unlabeled and [^{15}N]-labeled 5TMC fragments were obtained on a preparative scale in BL21(DE3) cells at 30°C for 20–21 h. A total of 18 mg of the 5TMC peptide (by weight) per liter of fermentation was recovered from the IBs. UV analysis indicated that at least 50% of this weight corresponded to 5TMC, whereas the remainder was most likely residual water and/or solvent molecules such as TFA or isopropanol. Analytical RP-HPLC analysis indicates that the 5TMC fractions are at least 96% pure. The [^{15}N]-uniformly labeled 5TMC was expressed in M9 media supplemented with [^{15}N]H_4Cl by induction at an OD_{600} of 1.0 with 0.25 m*M* IPTG in 500 mL of minimal medium (Figure 3C) to yield 9.4 mg (by weight) of the HPLC purified peptide with 96% [^{15}N]-incorporation as determined using MALDI-TOF analysis (Figure 3D) and the molecular weight obtained for unlabelled 5TMC as a standard.

The 4TMC fragment of Ste2p exhibited significantly lower expression than 5TMC as judged from peak intensities on HPLC analyses (compare Figure 3B and 4A) and was difficult to detect on Coomassie Blue stained gels (Figure 4B). Therefore, for 4TMC, optimal expression conditions were chosen based on Western blot analysis (Figure 4B). BL21(DE3) yielded relatively high expression of 4TMC in rich medium with 0.5 m*M* IPTG at 37°C for 4–6 h or at 30°C for 20–21 h. Both temperatures gave similar expression on a preparative scale, yielding 1.5–2 mg L^{-1} of culture of the HPLC purified 4TMC fragment. The molecular weight, as determined by MALDI-TOF, was in agreement with the calculated value (Figure 4C; Table I).

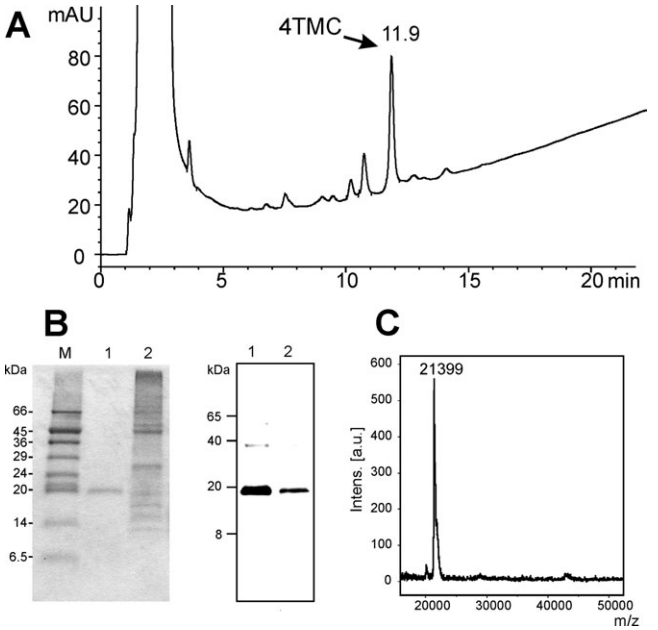

FIGURE 4 Biosynthesis of the Ste2p[T_{155}-L_{340}] (4TMC). (A) HPLC chromatogram of 4TMC IBs expressed in BL21(DE3) cells, LB medium with 0.5 m*M* IPTG at 30°C for 21 h. The HPLC column was Zorbax 300SB-C3 (4.6 × 150 mm; 3.5-μm). The HPLC gradient was from 50 to 88% eluent B (90% acetonitrile/10% isopropanol/0.1% TFA) where eluent A was 90% water/10% isopropanol/0.1% TFA. (B) Coomassie Blue stained gel (left panel) and Western Blot (right panel) of the isolated IBs (Lane 2) and HPLC purified 4TMC (lane 1). Lane M, SigmaMarker™ Low Range protein markers. (C) Positive MALDI-TOF spectrum of HPLC purified 4TMC. Expected molecular weight is 21,375 Da.

The Cys-less 4TMC-His_6 (Ste2p[T_{155}-L_{340}], C252S) and 5TMC-His_6 (Ste2p[I_{120}-L_{340}], C252S) constructs with a hexahistidine tag at the C-terminus were biosynthesized by direct expression using plasmids generated from the template pBEC2[65] and the pET21a vector. Both constructs exhibited low expression compared to that found for 5TMC in BL21(DE3) cells in LB medium as indicated by Western blot analysis (Supporting Information Figure S3C). However, the expression of the constructs with the His tag at the C terminus was comparable with that of 4TMC bearing a N-terminal His-tag (Supporting Information Figure S3C).

CD Study of Four and Five C-Terminal TM Domain Constructs

As stated in the Introduction an important current goal is to reconstitute 2TMN in the context of the entire GPCR. Therefore, our biophysical and structure analyses concentrated mostly on 5TMC [Ste2p(I_{120}-L_{340})], which is a viable partner for pairing with 2TMN. The secondary structure of the 5TMC fragment was analyzed in organic-aqueous (TFE/H_2O

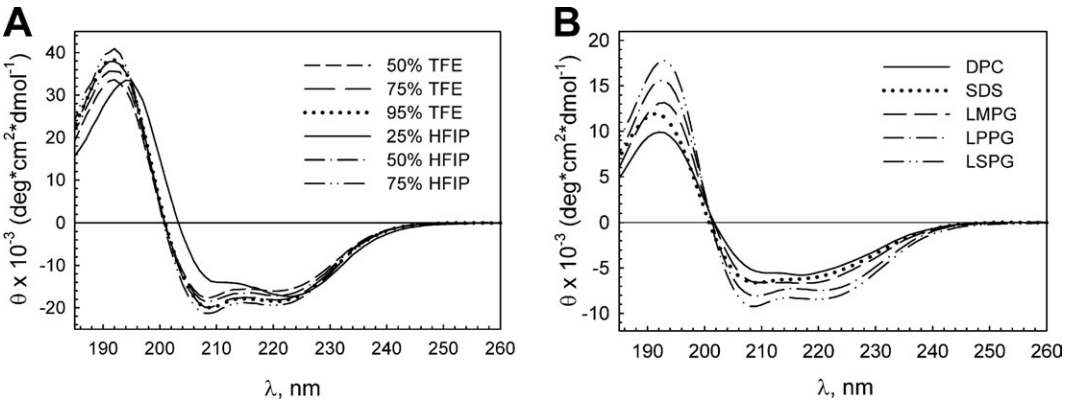

FIGURE 5 Far-UV CD spectra of Ste2p[I_{120}-L_{340}] (5TMC) in aqueous-organic solvents (A) and detergent micelles (B). Protein concentration was 10 μM. For the micelle study, the detergent-protein samples were dissolved in HFIP, lyophilized as described in Material and Methods and redissolved in 20 m*M* phosphate buffer, pH 5.6 containing 20 m*M* of the appropriate detergent.

and HFIP/H_2O) and micellar environments by CD (Figure 5). In organic solvents, the far-UV CD spectra had a maximum at around 192 nm (helical $\pi \rightarrow \pi^*$ transition), and minima at 222 nm (helical $n \rightarrow \pi^*$ transition) and 208 nm (helical $\pi \rightarrow \pi^*$ transition), indicating the expected helical content in the 5TMC structure. Using the mean residue ellipticity at 222 nm, we calculated (See Methods) that the fraction helix increased from 50% in 50% TFE/H_2O to 58% in 95% TFE/H_2O, and from 54% in 25% HFIP/H_2O to 62% in 75% HFIP/H_2O. These helicities are slightly higher than the 50% predicted helicity of this fragment, which is based on a rhodopsin-template model of Ste2p from the Smith group, analysis of Ste2p in TMpred[66] and inclusion of Helix 8, which was observed in our structural analysis of EL3-TM7-CT40 in DPC micelles.[55] The difference is not unexpected as we have shown previously that TFE:water lengthens the TM helical boundaries in Ste2p relative to those that are predicted[37,49] and that the helical content of the CT increases with increasing TFE (data not shown). In all organic-aqueous solutions, except for the 25% HFIP solution, the ratio of $[\theta_{222}]/[\theta_{208}]$ was around 0.90, close to the typical ratio for isolated helices ($\leqslant$0.86).[67] In 25% HFIP this ratio increased to 1.36, the absolute value of the ellipticity at 208 nm decreased considerably whereas that at 222 nm was nearly unchanged. The altered CD parameters suggest a change in the conformational distribution in this solvent system. Increasing the TFE or HFIP concentration from 50 to 75% resulted in a higher value of the negative ellipticity at 222 nm and, accordingly, an increase in the α-helical content together with decreasing random coil conformation. This is not surprising because these organic solvents are known to be inducers of helicity. Interestingly, further increase in the TFE concentration did not increase helicity and the 5TMC fragment displayed very similar CD profiles in 75 and 95% TFE. The greatest absolute ellipticity at 222 nm was observed in 75% HFIP, a stronger solvent and helix inducer with respect to TFE.[68,69]

After optimization of conditions for sample preparation (See Supporting Information Figure S4), CD analyses were carried out on 5TMC in micelles formed from detergents with various aliphatic tails and head groups (LMPG, LPPG, LSPG, DPC, and SDS). CD data on 5TMC indicated that samples prepared in LSPG (having the longest hydrophobic tail [17C]) had the greatest absolute values of the ellipticity at 222 and 193 nm (Figure 5B). We did not calculate percent helicity for 5TMC in the micellar samples because it is difficult to determine the exact concentration of the peptides in the micellar solutions. The increased $[\theta_{222}]$ values can correspond to increasing helicity or better incorporation into LSPG micelles than into other detergents. We believe the latter is much more likely for the system under investigation. Shortening a hydrophobic chain to 15C for LPPG and 13C for LMPG resulted in a progressive decrease in mean residue ellipticity at 193 and 222 nm. Changes in the head group for the detergents with 13C and 12C hydrocarbon tails (LMPG, SDS, and DPC) caused small variations in the CD curves of 5TMC (Figure 5B).

Using the same CD conditions and criteria, LPPG was found to be the best detergent for 4TMC (Figure 6). Lengthening or shortening of the acyl chain led to decreasing absolute ellipticity values. As with 5TMC, in DPC 4TMC showed the lowest values for peaks associable with $\pi \rightarrow \pi^*$ and $n \rightarrow \pi^*$ transitions and had a $[\theta_{222}]/[\theta_{208}]$ ratio around one (1.05). The CD screening allowed us to establish appropriate protocols for reconstitution of these sizable GPCR fragments and

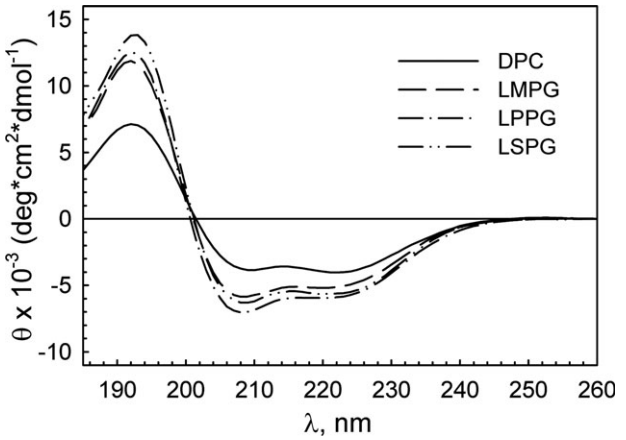

FIGURE 6 Far-UV CD spectra of Ste2p[T_{155}-L_{340}] (4TMC) in 20 m*M* phosphate buffer, pH 5.6 containing 20 m*M* of the appropriate detergent. 4TMC concentration was 10 μM.

for identifying the best detergent for further biophysical and structural investigations.

NMR Analysis of [[^{15}N]]-Labeled 5TMC [Ste2p(I_{120}-L_{340})]

One ultimate goal of studies on receptor fragments is to obtain high-resolution structural information. Accordingly, we measured [^{15}N,^{1}H]-HSQC spectra of [^{15}N]-uniformly labeled 5TMC in membrane mimetic organic-aqueous media (TFE-d_2/H_2O or HFIP-d_2/H_2O). These resulted in relatively high-concentration samples ($\sim$0.10–0.15 m*M*) that were needed for preliminary NMR analyses. [^{15}N,^{1}H]-HSQC and [^{15}N,^{1}H]-HSQC-TROSY spectra were run in TFE/H_2O at 45°C for 2 h. As judged by the number of resolved peaks, the line width, and the sensitivity, superior spectra were obtained in the HSQC-TROSY experiment (compare Figure 7A and Supporting Information Figure S5A). The same sample (Figure 7A) was checked by HSQC-TROSY after being held at 45°C for one (Supporting Information Figure S5B) and 2 weeks (Supporting Information Figure S5C) to evaluate stability. The [^{15}N,^{1}H]-HSQC-TROSY spectrum of the freshly prepared sample exhibited up to 90% of the expected cross-peaks, but the region between 7.6 and 8.2 ppm (Figure 7A) was severely crowded complicating peak assignment. After 1 week at 45°C, nearly all of the peaks still appeared in the spectrum but with reduced intensity probably due to some aggregation (Compare Figure 7A and Supporting Information Figure S5B). After 2 weeks, the intensity of certain peaks dropped significantly. Overall, the integrated intensities of the amide and aromatic proton region in the ^{1}H NMR spectrum retained about 70% of the initial value after 1-week sample incubation at 45°C and about 55% of the intensity after 2 weeks. MALDI-TOF analysis indicated slight degradation had occurred after 2 weeks (data not shown). The overall dispersion of the backbone amide peaks in the HSQC-TROSY spectrum was $\sim$1.6 ppm (from 7.3 to 8.9 ppm) in 50% TFE/H_2O. In 50% HFIP/H_2O (Figure 7B), this region was slightly wider $\sim$1.9 ppm (7.3–9.2 ppm) and peak overlap in the central region of the HSQC-TROSY spectrum was less severe compared to the TFE/H_2O solution. Peak dispersion in 80% TFE/H_2O (Figure 7C) was comparable to that of the HFIP spectrum. These differences may suggest that 5TMC has a slightly higher degree of order in 50% HFIP/H_2O and 80% TFE/H_2O than in 50% TFE/H_2O and are in agreement with the CD analysis.

Does 5TMC Integrate into Detergent Micelles? Fluorescence Studies

The 5TMC fragment contains a single Trp295 residue in the last TM domain (TM7) (Supporting Information Figure S1). Fluorescence spectroscopy, which provides information about tryptophan's local environment, was used to examine whether 5TMC integrated into micelles during the CD investigations. For comparison, spectra were measured in both 50% TFE/H_2O and LSPG micelles (Figure 8). The maximum fluorescence intensity was observed at 343 nm in 50% TFE/H_2O and at 314 nm in LSPG-containing phosphate buffer. The difference reflects the significantly less polar microenvironment of the Trp fluorophore in the LSPG micelle. The 29 nm shift suggests that the Trp295 of 5TMC is buried in a hydrophobic micellar core. A small reduction of fluorescence intensity was observed in LSPG micelles versus the organic-aqueous solution. This might reflect a more compact structure in LSPG that could result in additional quenching of Trp or the extent of incorporation into micelles, which might result in a lower than expected fluorophore concentration.

Is It Possible to Form Heterodimers to Reconstitute Ste2p?

In attempts to reassemble the entire Ste2p GPCR, fragments containing the first two (2TMN[48] and TM1-TM2) and last five (5TMC) TM domains were mixed, reconstituted into SDS micelles and analyzed by Western blot and MALDI-TOF. Only 5TMC had a His-tag so its monomer, oligomers, and heterodimer could be detected by Western blotting. 2TMN was invisible using this method unless it was heterodimerized with the 5TMC. The interactions were checked in phosphate buffer containing 20 or 200 m*M* SDS. In 20 m*M* SDS the 2 + 5 heterodimer MALDI signal was comparable with that from the 5TMC homodimer but both were very low compared with the 5TMC monomer (Supporting Information Figure S6). In 200 m*M* SDS more 5TMC homodimer

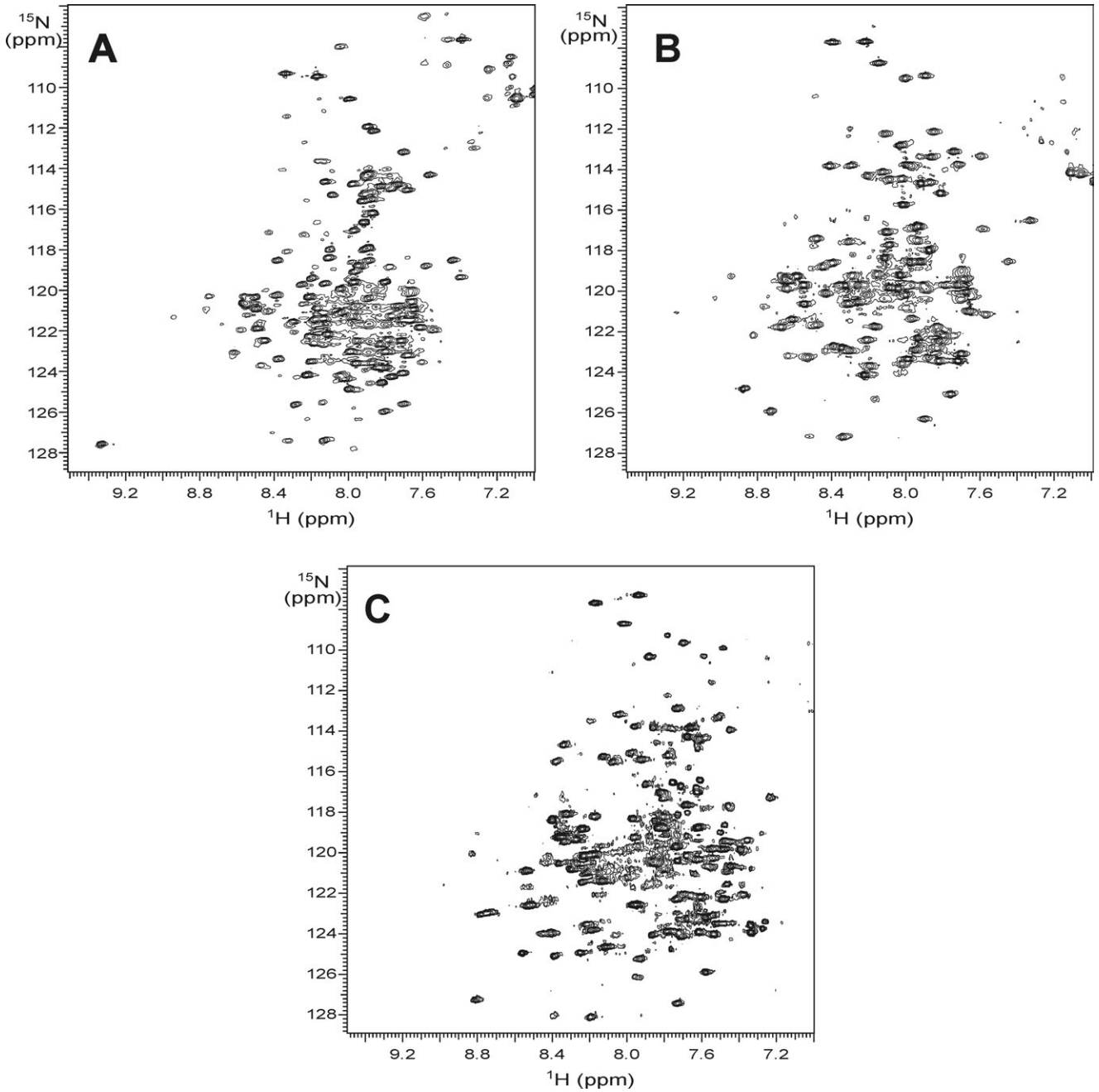

FIGURE 7 [^{15}N,^{1}H]-HSQC-TROSY spectra of Ste2p[I_{120}-L_{340}] (5TMC) in organic-aqueous solutions, 50%TFE-d_2/H_2O/0.05%TFA (A), 50%HFIP-d_2/H_2O/0.05%TFA (B), and 80%TFE-d_2/H_2O/0.02%TFA (C). The spectra were recorded during 2 h at 45°C.

was detected than the 2 + 5 heterodimer (data not shown). For further mixing experiments 20 m*M* SDS was chosen to increase the peptide to detergent ratio and thereby raise the probability of dimerization. Under these conditions peptide mixtures with various 2TMN/5TMC ratios (0.5/1, 1/1, 2/1, and 4/1) were analyzed. MALDI-TOF spectra showed that with increasing 2TMN content, the heterodimer signal was enhanced, whereas the 5TMC homodimer signal weakened (Supporting Information Figure S6). Western blot analysis of the Ste2p fragment mixtures separated by SDS-PAGE demonstrated a weak heterodimer band indicating weak interactions between the fragments under these conditions (Figure 9). We also tested interactions between another pair of Ste2p fragments, 3TMN[49] (TM1-TM3) and 4TMC, where only the 4TMC contained a His-tag. The study was carried out in 20 m*M* SDS micelles, the 3TMN/4TMC heterodimer

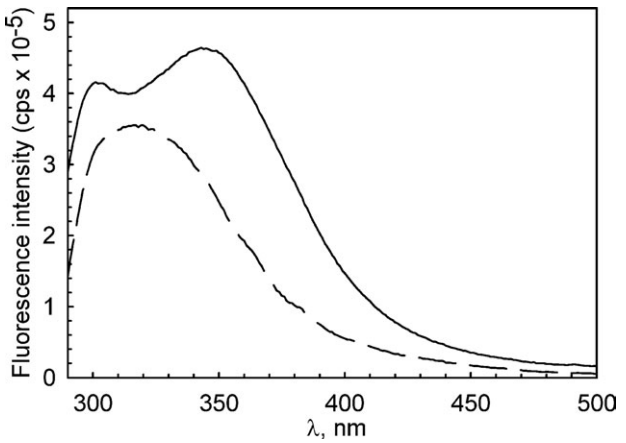

FIGURE 8 Fluorescence emission spectra of Ste2p[I_{120}-L_{340}] (5TMC) in 50%TFE/H_2O (solid line) and in 20 m*M* phosphate buffer, pH 5.6 containing 10 m*M* LSPG (dashed line). Protein concentration was 2.5 μM.

was found to have a stronger band in a Western blot (Figure 9B) with respect to the 2TMN/5TMC heterodimer and some heterooligomers were detected in this case. Increasing the relative concentration of the invisible 3TMN fragment resulted in less heterodimer (Figure 9B). This may be due to the shielding of the histidine tag in 4TMC and its oligodimers and heterodimers by 3TMN, thereby hindering detection of the 4TMC complexes. A similar but lesser effect was observed in the 2TMN/5TMN samples (Figure 9A).

DISCUSSION

Structural investigations of ligand-receptor interactions and receptor regulation require sufficient amounts of high-quality stable protein. The goal of this study was to develop a biosynthetic strategy for the isolation of mg quantities of large TM-containing fragments of a G protein-coupled receptor (Ste2p) in unlabeled and labeled forms for characterization by biophysical methods and for future reconstitution experiments with shorter fragments. The fusion protein approach has been extensively employed for the biosynthesis of soluble proteins, and TM peptides and proteins. Such target molecules have been obtained using expression systems with maltose-binding protein (MBP), thioredoxin (Trx), or fluorescent proteins as fusion partners.[70–75] Pertinent to one of the goals of the present investigation, the insertion of MBP at the N-terminus and Trx at the C-terminus has been reported to

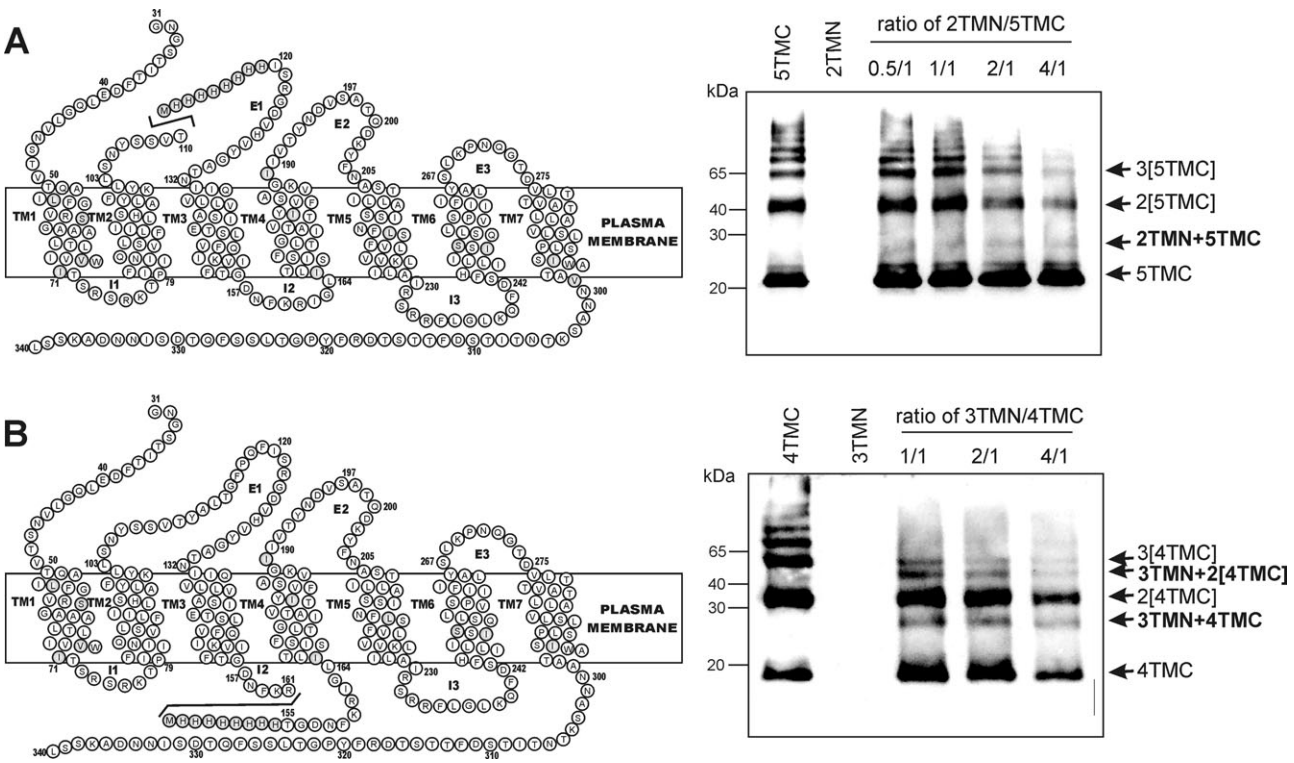

FIGURE 9 Western Blot analysis of mixtures of Ste2p fragments of different size. 2TMN + 5TMC (A) and 3TMN + 4TMC (B) in 20 m*M* SDS micelles. The fragments are illustrated in cartoon fashion at the left of each panel. A line indicates the break between the fragments. To the right of each panel are Western Blots of SDS-PAGE gels, which were probed for histidine tags. TM, transmembrane domain; E, extracellular loop; I, intracellular loop.

improve the expression of the rat neurotensin receptor NTS1[71] and the human peripheral cannabinoid receptor CB2.[75] These hydrophilic fusion partners increase the water solubility of the hydrophobic target proteins, improve their stability, and reduce their toxicity by promoting their overexpression and accumulation in IBs. In our laboratory, previous examination of different fusion systems[47] has convinced us that the TrpΔLE1413 polypeptide, initially used by Staley and Kim,[63] was the best fusion partner for Ste2p fragments and was useful for obtaining one, two or three TM domain segments.[45,47–49] Other groups have also used the TrpΔLE1413 fusion protein to biosynthesize large membrane protein fragments including fragments of the cannabinoid GPCR[31,76] and the HIV-1 protein Vpu.[77,78]

In the present communication, we report the biosynthesis of three constructs, containing four or five membrane-spanning Ste2p domains. Our biosynthetic experiments tested two different protocols for preparing receptor fragments containing 4 and 5 TMs: (1) our standard TrpΔLE fusion protein protocol, which requires processing by cyanogen bromide and (2) a direct expression approach that simplifies the overall method by eliminating the intermediate fusion protein purification and cleavage with the highly toxic cyanogen bromide reagent. The best heterologous expression for the fusion and direct expression constructs transformed into various BL21 *E. coli* strains was found in BL21(DE3) cells at 30°C. As found for shorter TrpΔLE-fusion Ste2p fragments,[48,49] the TrpΔLE-4TMN fusion protein expressed well in BL21-AI cells in M9 medium, but had lower expression in LB. We also observed that both the OD_{600} of the induction and the temperature of the culture could have a strong influence on the level of expression in both LB and M9. The same dependence has been reported previously for minimal media[26,51] where best expression was induced when the OD_{600} was >1. The expression temperature of 30°C was favorable for all of the Ste2p fragments in this study.

The Ste2p fragments biosynthesized under our best conditions accumulated in IBs and were analyzed by RP-HPLC with a linear gradient containing a high content of organic solvents (50–88% acetonitrile in water with 10% isopropanol and 0.1% TFA for 30 min) at a temperature of 60°C. These harsh HPLC conditions were required for elution of highly hydrophobic 4TMN-FP, 4TMC, and 5TMC. In comparison to 4TMC, the longer retention time observed for the target 4TMN fragment is not surprising because 4TMC has a long hydrophilic tail and 4TMN contains an aggregation inducing first extracellular loop. RP-HPLC in organic solvents undoubtedly leads to unfolded peptides. Nevertheless, these solvents were found to be necessary to dissolve the expressed proteins, which accumulate in IBs. Although others have tried to use metal ion affinity chromatography to isolate membrane fragments we have not had any success with this approach and have experienced large losses of protein. Despite the treatments, we found the Ste2p fragments we isolated could be integrated into micelles and were suitable for biophysical analysis. When reconstitution to form the entire receptor is attempted, it is likely that mixed micellar media similar to those used for GPCR crystallization may be necessary.

A significant variation in the amount of the directly expressed 4TMC (1.5–2 mg/L) and 5TMC (18–20 mg/L) polypeptides was observed. There are several possible explanations for this large difference. The 5TMC sequence starts from the first extracellular loop, and the 4TMC fragment begins at the second intracellular loop. This difference may affect the folding and stability of these proteins and thereby the final yield. To evaluate the His-tag influence on the level of protein expression of the fragments, the extra His residues were moved to the C-terminus, which is expected to have a lower effect on the folding during expression. The change in the location of the His-tag did not improve the expression; both the 5TMC-His_6 and 4TMC-His_6 fragments with the C-terminal His-tag were produced at amounts lower than 5TMC with the N-terminal His-tag (Supporting Information Figure S3C). Nevertheless, the results suggest a contribution of the N-terminal polyhistidine region to the high expression of the target 5TMC peptide.

A major current goal of our laboratory is to conduct high-resolution studies on 2TMN in the context of a reconstituted receptor. This requires us to reassemble the receptor from 2TM and 5TM containing fragments. To characterize the biophysical properties of the 5TM containing fragment of Ste2p, further spectroscopic investigations were focused on the largest recombinant 5TMC construct, containing an N-terminal octahistidine tag. This GPCR domain was biosynthesized in unlabeled and [^{15}N]-uniformly labeled forms in multimilligram quantities with high homogeneity as estimated from a comprehensive analysis by SDS-PAGE, MALDI-TOF, and HPLC. CD and heterodimer formation were also evaluated with the 4TMC construct. Solubilization of the hydrophobic proteins was achieved in various membrane-mimetic systems including organic-aqueous mixtures with TFE or HFIP, and detergent micelles. TFE and HFIP are well known to stabilize and induce helical secondary structure of peptides and proteins. As suggested by molecular dynamics simulations,[79,80] these fluorocarbon alcohols concentrate around the peptide and form a matrix that displaces water and, consequently, promotes intramolecular hydrogen bonds stabilizing a helical secondary structure. The putatively isotropic solvents interact only weakly with apolar residues

and, unlike many denaturing agents, should not interrupt the internal interactions. At high concentration, the more extensive solvent shell can impair tertiary and quaternary contacts.[81] Thus, it is not surprising that we observed enhanced 5TMC helicity in the presence of TFE and HFIP with the latter demonstrating stronger inducer characteristics. CD revealed that at high concentrations of TFE or HFIP, the 5TMC is ~60% α-helical, which agrees well with predictions.

In micelles, we observed decreasing 5TMC ellipticities as the length of the acyl chain of the detergent decreased, with the highest values found in LSPG micelles. In this peptide-detergent complex, the long hydrophobic tail may extensively bury the putative TM regions of 5TMC in the micellar core. Detergents with shorter acyl tails like LMPG, SDS, or DPC form micelles of a size that may not fully incorporate the large peptide structure into the hydrocarbon core and protect it from the aqueous environment. In such systems, interpeptide hydrophobic contacts may be increased leading to the destabilization of secondary structure and aggregation, both of which would result in decreased helical CD parameters. Comparative CD analysis revealed a correlation between the size of a membrane fragment and the length of the detergent acyl chain that best stabilizes the peptide. Constructs of larger size demonstrated higher ellipticity in detergents with a longer acyl chain, whereas the smaller peptide fragment was most helical in a detergent with a shorter hydrocarbon tail (Supporting Information Figure S4D). Although it is not clear whether the higher ellipticity is due to increase in secondary structure or in the concentration of the peptide, the study clearly shows that the hydrocarbon chain length of the detergent is a critical factor in achieving optimum conditions for biophysical studies on Ste2p fragments. With very large fragments such as 5TMC and 4TMC micelles may not represent an optimum membrane mimetic and better results may be obtained with bicelles or bilayers. Such studies are beyond the scope of this analysis.

The fluorescence study of the single Trp295 near the end of the TM7 domain of 5TMC revealed a blue shift of the emission maximum wavelength (29 nm) in LSPG micelles compared with TFE/H_2O solutions. Organic-aqueous membrane mimetics and detergents, in principle, form a hydrophobic contact solvation shell around TM regions of proteins thereby shielding them from water molecules. However, micellar media are better at excluding peptide-water contacts leading to less flexibility and better protection of the buried peptide chain. The fluorescence λ_{max} values confirm the strong shielding of this Trp in the micelle and its higher exposure in the organic-aqueous medium. In support of this conclusion, the same blue shift has been detected for TM peptides in SDS micelles versus aqueous buffer[82] or in DPC micelles versus 30% TFE/H_2O.[83] However in these latter studies, an increase in fluorescence intensity, which was not observed in our case, was reported.

Analysis of HSQC-TROSY NMR spectra of 5TMC in 50% TFE/H_2O solution at 45°C suggests some aggregation and loss of the protein from solution over time. However, the observed stability of the spectrum for 1–2 weeks indicates that sample stability in fluoroalcohols, as a membrane mimetic environment, should be sufficient to measure the series of 3D NMR spectra necessary for assignments and structure determination. Given the status of NMR studies on intact GPCRs, it would be valuable to work with a reconstituted receptor where some domains are NMR visible and others are NMR silent. Therefore, we evaluated whether conditions could be developed to reconstitute 2TMN and 5TMC or 3TMN and 4TMC to form a heterodimer. Mixtures of these peptides in the presence of SDS micelles exhibited only weak interactions and heterodimer signals on Western blots and in MALDI-TOF spectra. This is likely because to obtain heterodimerization one must use relatively low detergent to peptide ratios (20 m*M* SDS instead of 200 m*M* SDS) so that both components will enter one micelle. Although these conditions should favor peptide/peptide contact, it is apparently difficult to form selectively the desired heterodimer. We cannot rule out the possibility, however, that the methods used to study heterodimerization (SDS-PAGE; MALDI-TOF) disrupt their formation. In view of these concerns, it is encouraging that the heterodimer MALDI signals are comparable to those from the homodimers, and that we see more heterodimer as the excess of one of the components is increased. Additional attempts to reconstitute the heterodimers for NMR evaluation might benefit from bicelles where the fragments would integrate into a planar environment that can assist these large fragments to fold into a heptahelical bundle. Nevertheless, the overall conclusion is that spontaneous reconstitution will not be efficient enough for NMR studies in micellar solutions. Currently we are developing conditions for the Guided Reconstitution of the 2TMN fragment with 5TMC using heterodisulfide formation. This covalent linkage should stabilize the reconstituted receptor and drive the equilibrium to favor its formation.

In summary, successful isolation of fragments of a GPCR containing four and five TM domains has been obtained on a multimilligram scale. Conditions have been optimized for biophysical characterization of the fragments by CD and fluorescence and for structural analysis by NMR. The NMR results show promise for a structural analysis of 5TMC a 230-residue peptide in aqueous TFE or HFIP solutions. The methodology that has been developed will enable production

and isolation of complimentary partners, 5TMC for 2TMN and 4TMC for 3TMN, needed for the reconstitution of the intact receptor. Studies on the fragments alone and in the context of the reassembled Ste2p should provide insights into the three dimensional structure and mechanism of action of the receptor domains.

The authors are grateful for help and advice received from Professor Mark Dumont and his research staff at the University of Rochester in the form of plasmids coding for Ste2p and from Sarah Kauffmann and Melinda Hauser for help in sequencing and evaluating the Ste2p(A299V) plasmid. Mohammed Bhuiyan also aided us at various points in this project.

REFERENCES

1. Fredriksson, R.; Hoglund, P. J.; Gloriam, D. E.; Lagerstrom, M. C.; Schioth, H. B. FEBS Lett 2003, 554, 381–388.
2. Lundstrom, K. H.; Chiu, M. L. G Protein-Coupled Receptors in Drug Discovery. CRC Press: Boca Raton, 2006.
3. Vassart, G.; Costagliola, S. Nat Rev Endocrinol 2011, 7, 362–372.
4. Filmore, D. Mod Drug Discov 2004, 7, 24–28.
5. Palczewski, K.; Kumasaka, T.; Hori, T.; Behnke, C. A.; Motoshima, H.; Fox, B. A.; Le Trong, I.; Teller, D. C.; Okada, T.; Stenkamp, R. E.; Yamamoto, M.; Miyano, M. Science 2000, 289, 739–745.
6. Cherezov, V.; Rosenbaum, D. M.; Hanson, M. A.; Rasmussen, S. G.; Thian, F. S.; Kobilka, T. S.; Choi, H. J.; Kuhn, P.; Weis, W. I.; Kobilka, B. K.; Stevens, R. C. Science 2007, 318, 1258–1265.
7. Rasmussen, S. G.; Choi, H. J.; Rosenbaum, D. M.; Kobilka, T. S.; Thian, F. S.; Edwards, P. C.; Burghammer, M.; Ratnala, V. R.; Sanishvili, R.; Fischetti, R. F.; Schertler, G. F.; Weis, W. I.; Kobilka, B. K. Nature 2007, 450, 383–387.
8. Warne, T.; Serrano-Vega, M. J.; Baker, J. G.; Moukhametzianov, R.; Edwards, P. C.; Henderson, R.; Leslie, A. G.; Tate, C. G.; Schertler, G. F. Nature 2008, 454, 486–491.
9. Park, J. H.; Scheerer, P.; Hofmann, K. P.; Choe, H. W.; Ernst, O. P. Nature 2008, 454, 183–187.
10. Jaakola, V. P.; Griffith, M. T.; Hanson, M. A.; Cherezov, V.; Chien, E. Y.; Lane, J. R.; Ijzerman, A. P.; Stevens, R. C. Science 2008, 322, 1211–1217.
11. Wu, B.; Chien, E. Y.; Mol, C. D.; Fenalti, G.; Liu, W.; Katritch, V.; Abagyan, R.; Brooun, A.; Wells, P.; Bi, F. C.; Hamel, D. J.; Kuhn, P.; Handel, T. M.; Cherezov, V.; Stevens, R. C. Science 2010, 330, 1066–1071.
12. Chien, E. Y.; Liu, W.; Zhao, Q.; Katritch, V.; Han, G. W.; Hanson, M. A.; Shi, L.; Newman, A. H.; Javitch, J. A.; Cherezov, V.; Stevens, R. C. Science 2010, 330, 1091–1095.
13. Shimamura, T.; Shiroishi, M.; Weyand, S.; Tsujimoto, H.; Winter, G.; Katritch, V.; Abagyan, R.; Cherezov, V.; Liu, W.; Han, G. W.; Kobayashi, T.; Stevens, R. C.; Iwata, S. Nature 2011, 475, 65–70.
14. Xu, F.; Wu, H.; Katritch, V.; Han, G. W.; Jacobson, K. A.; Gao, Z. G.; Cherezov, V.; Stevens, R. C. Science 2011, 332, 322–327.
15. Hanson, M. A.; Roth, C. B.; Jo, E.; Griffith, M. T.; Scott, F. L.; Reinhart, G.; Desale, H.; Clemons, B.; Cahalan, S. M.; Schuerer, S. C.; Sanna, M. G.; Han, G. W.; Kuhn, P.; Rosen, H.; Stevens, R. C. Science 2012, 335, 851–855.
16. Manglik, A.; Kruse, A. C.; Kobilka, T. S.; Thian, F. S.; Mathiesen, J. M.; Sunahara, R. K.; Pardo, L.; Weis, W. I.; Kobilka, B. K.; Granier, S. Nature 2012.
17. Kruse, A. C.; Hu, J.; Pan, A. C.; Arlow, D. H.; Rosenbaum, D. M.; Rosemond, E.; Green, H. F.; Liu, T.; Chae, P. S.; Dror, R. O.; Shaw, D. E.; Weis, W. I.; Wess, J.; Kobilka, B. K. Nature 2012, 482, 552–556.
18. Wu, H.; Wacker, D.; Mileni, M.; Katritch, V.; Han, G. W.; Vardy, E.; Liu, W.; Thompson, A. A.; Huang, X. P.; Carroll, F. I.; Mascarella, S. W.; Westkaemper, R. B.; Mosier, P. D.; Roth, B. L.; Cherezov, V.; Stevens, R. C. Nature 2012, 485, 327–332.
19. Granier, S.; Manglik, A.; Kruse, A. C.; Kobilka, T. S.; Thian, F. S.; Weis, W. I.; Kobilka, B. K. Nature 2012, 485, 400–404.
20. Thompson, A. A.; Liu, W.; Chun, E.; Katritch, V.; Wu, H.; Vardy, E.; Huang, X. P.; Trapella, C.; Guerrini, R.; Calo, G.; Roth, B. L.; Cherezov, V.; Stevens, R. C. Nature 2012, 485, 395–399.
21. Bockaert, J.; Pin, J. P. EMBO J 1999, 18, 1723–1729.
22. Horn, F.; Bettler, E.; Oliveira, L.; Campagne, F.; Cohen, F. E.; Vriend, G. Nucleic Acids Res 2003, 31, 294–297.
23. Bissantz, C. J Recept Signal Transduct Res 2003, 23, 123–153.
24. Cavasotto, C. N.; Orry, A. J.; Murgolo, N. J.; Czarniecki, M. F.; Kocsi, S. A.; Hawes, B. E.; O'Neill, K. A.; Hine, H.; Burton, M. S.; Voigt, J. H.; Abagyan, R. A.; Bayne, M. L.; Monsma, F. J., Jr. J Med Chem 2008, 51, 581–588.
25. Tian, C.; Breyer, R. M.; Kim, H. J.; Karra, M. D.; Friedman, D. B.; Karpay, A.; Sanders, C. R. J Am Chem Soc 2005, 127, 8010–8011.
26. Berger, C.; Ho, J. T.; Kimura, T.; Hess, S.; Gawrisch, K.; Yeliseev, A. Protein Expr Purif 2010, 70, 236–247.
27. Park, S. H.; Casagrande, F.; Chu, M.; Maier, K.; Kiefer, H.; Opella, S. J. Biochim Biophys Acta 2012, 1818, 584–591.
28. Gautier, A.; Mott, H. R.; Bostock, M. J.; Kirkpatrick, J. P.; Nietlispach, D. Nat Struct Mol Biol 2010, 17, 768–774.
29. Reckel, S.; Gottstein, D.; Stehle, J.; Lohr, F.; Verhoefen, M. K.; Takeda, M.; Silvers, R.; Kainosho, M.; Glaubitz, C.; Wachtveitl, J.; Bernhard, F.; Schwalbe, H.; Guntert, P.; Dotsch, V. Angew Chem Int Ed Engl 2011, 50, 11942–11946.
30. Tikhonova, I. G.; Costanzi, S. Curr Pharm Des 2009, 15, 4003–4016.
31. Zheng, H.; Zhao, J.; Sheng, W.; Xie, X. Q. Biopolymers 2006, 83, 46–61.
32. Zou, C.; Naider, F.; Zerbe, O. J Biomol NMR 2008, 42, 257–269.
33. Tyukhtenko, S.; Tiburu, E. K.; Deshmukh, L.; Vinogradova, O.; Janero, D. R.; Makriyannis, A. Biochem Biophys Res Commun 2009, 390, 441–446.
34. Tiburu, E. K.; Tyukhtenko, S.; Zhou, H.; Janero, D. R.; Struppe, J.; Makriyannis, A. AAPS J 2011, 13, 92–98.
35. Kocherla, H.; Marino, J.; Shao, X.; Graf, J.; Zou, C.; Zerbe, O. Chem Biochem 2012, 13, 818–828.
36. Neumoin, A.; Cohen, L. S.; Arshava, B.; Tantry, S.; Becker, J. M.; Zerbe, O.; Naider, F. Biophys J 2009, 96, 3187–3196.
37. Cohen, L. S.; Arshava, B.; Neumoin, A.; Becker, J. M.; Guntert, P.; Zerbe, O.; Naider, F. Biochim Biophys Acta 2011, 1808, 2674–2684.
38. Kobilka, B. K.; Kobilka, T. S.; Daniel, K.; Regan, J. W.; Caron, M. G.; Lefkowitz, R. J. Science 1988, 240, 1310–1316.
39. Maggio, R.; Vogel, Z.; Wess, J. FEBS Lett 1993, 319, 195–200.
40. Schoneberg, T.; Liu, J.; Wess, J. J Biol Chem 1995, 270, 18000–18006.
41. Ridge, K. D.; Lee, S. S.; Abdulaev, N. G. J Biol Chem 1996, 271, 7860–7867.

42. Martin, N. P.; Leavitt, L. M.; Sommers, C. M.; Dumont, M. E. Biochemistry 1999, 38, 682–695.
43. Scarselli, M.; Armogida, M.; Chiacchio, S.; DeMontis, M. G.; Colzi, A.; Corsini, G. U.; Maggio, R. Eur J Pharmacol 2000, 397, 291–296.
44. Burkholder, A. C.; Hartwell, L. H. Nucleic Acids Res 1985, 13, 8463–8475.
45. Arevalo, E.; Estephan, R.; Madeo, J.; Arshava, B.; Dumont, M.; Becker, J. M.; Naider, F. Biopolymers 2003, 71, 516–531.
46. Naider, F.; Estephan, R.; Englander, J.; Suresh Babu, V. V.; Arevalo, E.; Samples, K.; Becker, J. M. Biopolymers 2004, 76, 119–128.
47. Estephan, R.; Englander, J.; Arshava, B.; Samples, K. L.; Becker, J. M.; Naider, F. Biochemistry 2005, 44, 11795–11810.
48. Cohen, L. S.; Arshava, B.; Estephan, R.; Englander, J.; Kim, H.; Hauser, M.; Zerbe, O.; Ceruso, M.; Becker, J. M.; Naider, F. Biopolymers 2008, 90, 117–130.
49. Caroccia, K. E.; Estephan, R.; Cohen, L. S.; Arshava, B.; Hauser, M.; Zerbe, O.; Becker, J. M.; Naider, F. Biopolymers 2011, 96, 757–771.
50. Kunkel, T. A. Proc Natl Acad Sci USA 1985, 82, 488–492.
51. Marley, J.; Lu, M.; Bracken, C. J Biomol NMR 2001, 20, 71–75.
52. Naider, F. In Methods in Molecular Biology; Fields, G. B., Ed.; Humana Press: Totowa, NJ, 2006.
53. Schagger, H.; von Jagow, G. Anal Biochem 1987, 166, 368–379.
54. Naider, F.; Ding, F. X.; VerBerkmoes, N. C.; Arshava, B.; Becker, J. M. J Biol Chem 2003, 278, 52537–52545.
55. Neumoin, A.; Arshava, B.; Becker, J.; Zerbe, O.; Naider, F. Biophys J 2007, 93, 467–482.
56. Xie, H.; Ding, F. X.; Schreiber, D.; Eng, G.; Liu, S. F.; Arshava, B.; Arevalo, E.; Becker, J. M.; Naider, F. Biochemistry 2000, 39, 15462–15474.
57. Greenfield, N.; Fasman, G. D. Biochemistry 1969, 8, 4108–4116.
58. Kay, L. E.; Keifer, P.; Saarinen, T. J Am Chem Soc 1992, 114, 10663–10665.
59. Weigelt, J. J Am Chem Soc 1998, 120, 10778–10779.
60. Wishart, D. S.; Bigam, C. G.; Yao, J.; Abildgaard, F.; Dyson, H. J.; Oldfield, E.; Markley, J. L.; Sykes, B. D. J Biomol NMR 1995, 6, 135–140.
61. Markley, J. L.; Bax, A.; Arata, Y.; Hilbers, C. W.; Kaptein, R.; Sykes, B. D.; Wright, P. E.; Wuthrich, K. Eur J Biochem 1998, 256, 1–15.
62. Miozzari, G. F.; Yanofsky, C. J Bacteriol 1978, 133, 1457–1466.
63. Staley, J. P.; Kim, P. S. Protein Sci 1994, 3, 1822–1832.
64. Martin, N. P.; Celic, A.; Dumont, M. E. J Mol Biol 2002, 317, 765–788.
65. Hauser, M.; Kauffman, S.; Lee, B. K.; Naider, F.; Becker, J. M. J Biol Chem 2007, 282, 10387–10397.
66. Hofmann, K.; Stoffel, W. Biol Chem Hoppe Seyler 1993, 374.
67. Zhou, N. E.; Kay, C. M.; Hodges, R. S. J Biol Chem 1992, 267, 2664–2670.
68. Hirota, N.; Mizuno, K.; Goto, Y. Protein Sci 1997, 6, 416–421.
69. Contreras, M. A.; Haack, T.; Royo, M.; Giralt, E.; Pons, M. Lett Peptide Sci 1997, 4, 29–39.
70. Grisshammer, R.; Tate, C. G. Q Rev Biophys 1995, 28, 315–422.
71. Tucker, J.; Grisshammer, R. Biochem J 1996, 317 (Pt 3), 891–899.
72. Therien, A. G.; Glibowicka, M.; Deber, C. M. Protein Expr Purif 2002, 25, 81–86.
73. Yin, D.; Gavi, S.; Shumay, E.; Duell, K.; Konopka, J. B.; Malbon, C. C.; Wang, H. Y. Biochem Biophys Res Commun 2005, 329, 281–287.
74. Harding, P. J.; Attrill, H.; Ross, S.; Koeppe, J. R.; Kapanidis, A. N.; Watts, A. Biochem Soc Trans 2007, 35, 760–763.
75. Yeliseev, A.; Zoubak, L.; Gawrisch, K. Protein Expr Purif 2007, 53, 153–163.
76. Zheng, H.; Zhao, J.; Wang, S.; Lin, C. M.; Chen, T.; Jones, D. H.; Ma, C.; Opella, S.; Xie, X. Q. J Pept Res 2005, 65, 450–458.
77. Marassi, F. M.; Ma, C.; Gratkowski, H.; Straus, S. K.; Strebel, K.; Oblatt-Montal, M.; Montal, M.; Opella, S. J. Proc Natl Acad Sci USA 1999, 96, 14336–14341.
78. Kochendoerfer, G. G.; Jones, D. H.; Lee, S.; Oblatt-Montal, M.; Opella, S. J.; Montal, M. J Am Chem Soc 2004, 126, 2439–2446.
79. Roccatano, D.; Colombo, G.; Fioroni, M.; Mark, A. E. Proc Natl Acad Sci USA 2002, 99, 12179–12184.
80. Roccatano, D.; Fioroni, M.; Zacharias, M.; Colombo, G. Protein Sci 2005, 14, 2582–2589.
81. Bordag, N.; Keller, S. Chem Phys Lipids 2010, 163, 1–26.
82. Tulumello, D. V.; Deber, C. M. Biochemistry 2009, 48, 12096–12103.
83. Tiburu, E. K.; Tyukhtenko, S.; Deshmukh, L.; Vinogradova, O.; Janero, D. R.; Makriyannis, A. Biochem Biophys Res Commun 2009, 384, 243–248.